energies

MDPI

Article

Slow Pyrolysis of De-Oiled Rapeseed Cake: Influence of Pyrolysis Parameters on the Yield and Characteristics of the Liquid Obtained

Yue Wang [1], Yuanjiang Zhao [2] and Changwei Hu [1,*]

[1] Key Laboratory of Green Chemistry and Technology, Ministry of Education, College of Chemistry, Sichuan University, Wangjiang Road 29, Chengdu 610064, China; yue_wang@stu.scu.edu.cn
[2] Key Laboratory of Macromolecular Synthesis and Functionalization, Ministry of Education, Department of Polymer Science and Engineering, Zhejiang University, Hangzhou 310027, China; 11829034@zju.edu.cn
* Correspondence: changweihu@scu.edu.cn; Tel.: +86-28-85411105

Abstract: Pyrolysis of biomass converts all components into liquid, gaseous, and solid products without the need for component separation. However, the composition of liquid products from lignocellulosic biomass is usually complex and difficult to upgrade. Slow pyrolysis of de-oiled rapeseed cake, an agricultural waste from the rapeseed pressing process, was carried out for liquid and solid fuel production. The maximum yield of bio-oil obtained was 51.6 wt.% under the optimized conditions. The HHV of the bio-oil, containing mainly acids, hydrocarbons, esters, and alcohols, was 32.82 MJ·kg^{-1}, similar to that of bio-diesel, to be promising in downstream upgrading because the fuel properties such as higher caloric value, limited moisture content, as well as neutral pH value, were close to commercial bio-diesel. The gaseous fraction mainly consisted of CO, C_1, C_2 hydrocarbons, H_2, and CO_2, and the corresponding LHV reached 7.63 MJ·Nm^{-3}. The yield of bio-chars declined from 41.8 wt.% at 400 °C to 28.8 wt.% at 800 °C, whereas the corresponding HHV varied from 29.03 MJ·kg^{-1} to 30.14 MJ·kg^{-1}, comparative to coal, indicating a promising candidate for solid fuels or functional carbon. The liquid product shows promise as feedstock for producing high-quality fuel.

Keywords: de-oiled rapeseed cake; bio-oil; pyrolysis parameters

check for updates

Citation: Wang, Y.; Zhao, Y.; Hu, C. Slow Pyrolysis of De-Oiled Rapeseed Cake: Influence of Pyrolysis Parameters on the Yield and Characteristics of the Liquid Obtained. *Energies* **2024**, *17*, 612. https://doi.org/10.3390/en17030612

Academic Editors: Pingping Luo, Guangwei Huang, Binaya Kumar Mishra and Mohd Remy Rozainy Bin Mohd Arif Zainol

Received: 3 January 2024
Revised: 20 January 2024
Accepted: 24 January 2024
Published: 26 January 2024

1. Introduction

Energy is indispensable for the development of the global economy and the social activities of human society, while over-reliance on fossil fuels has resulted in severe issues of energy shortage and environmental concerns worldwide [1–4]. With the backdrop of global carbon emission restrictions, there is an increasing focus on the detrimental effects of traditional energy sources, such as fossil fuel, on the ecological environment [2,3]. Hence, within the realm of energy research, a significant focus lies in the quest for alternative energy sources that have minimal environmental repercussions. Biomass, which is a renewable and promising resource for addressing the climate crisis and reducing anthropogenic carbon dioxide (CO_2) emissions, has been widely recognized as a key alternative in achieving global carbon neutrality [2,3,5,6]. Furthermore, it is widely regarded as having significant potential in addressing energy shortages via thermochemical conversion. As an effective process for the valorization of biomass, pyrolysis can convert holocellulose, lignin, protein, and other biomass components into bio-oil, biochar, and bio-gas (syngas), improving energy density or obtain new materials [4,7–11].

Rather than traditional pyrolysis focusing on a single product, pyrolysis poly-generation aims to maximize the value of given feedstock in a more diverse and environmentally friendly approach to fuels, chemicals, and materials, which has been extensively researched and is considered to be a promising process for biomass valorization [12–14]. Chen et al. [12]

investigated the torrefaction of agriculture straws such as cotton stalk and corn stalk and its effects on product properties obtained under the optimal conditions of related pyrolytic poly-generation. Brigljević et al. [15] carried out a comprehensive feasibility assessment of one pyrolysis poly-generation process on *Saccharina japonica* (one kind of brown seaweed) for effective valorization of 3rd generation biofuel feedstock. Lei et al. [16] launched research on design and optimization in the utilization of municipal solid waste disposal through a poly-generation system integrating pyrolysis, incineration, and anaerobic digestion processes. Moreover, the industrial demonstration application of slow pyrolysis poly-generation technology, utilizing agroforest residues for rural heating, has advanced significantly in China, where Cong et al. [17] evaluated the technical characteristics and adaptability, suggesting that the progress in industrialization satisfied the demands that the involved plants be sustainable and capable of being replicated.

Woody biomass pyrolysis resulted in a low HHV value of 16–19 MJ·kg^{-1} with a bio-oil yield of 42.4–60.9 wt.%, far lower than that of commercial fuels [18–20]. Pyrolysis of agriculture wastes such as rice straw, wheat straw, switchgrass, and sugarcane usually leads to a lower yield of bio-oils (25.6–46 wt.%) with HHV ranging from 13 to 24 MJ·kg^{-1}, also much lower than that of fossil fuel. Algae consist of protein, fatty acids, holocellulose, and lignin, different from conventional lignocellulosic biomass, and the pyrolysis of this kind of biomass could yield more than 65 wt.% bio-oil but with a poor HHV value of 25.7 MJ·kg^{-1} [21,22]. Seed hulls such as sunflower seed hulls and soybean dregs are another kind of biomass source with acceptable availability, and the pyrolysis of these merely leads to poor properties of bio-oils (either acceptable HHV values but with undesirable bio-oil yield, such as 34 wt.% of bio-oil yield with HHV of 32.2 MJ·kg^{-1}, or acceptable bio-oil yield but with poor HHV value such as 40.3–47.9 wt.% of bio-oil with HHV of 12.3–15.3 MJ·kg^{-1}, respectively [20,23]. Thus, the bio-oil from pyrolysis of these feedstocks mentioned is difficult to upgrade to high-quality fuel because of their low HHV value, high moisture content, complex composition, etc. Given the vital significance of comprehending the attributes of bio-oil, particularly its relationship with the biomass source, it is imperative to reexamine research endeavors focusing on bio-oil production through the pyrolysis of diverse biomass varieties. Moreover, a comparison of the properties of bio-oils with fossil fuels is indispensable as well. Thus, suitable feedstocks are urgently needed to be investigated. Rapeseed ranks the third most important oilseed globally, following soybeans and cottonseed, with a production of 86.37 MMT and contributing to 11% of the total worldwide oilseed production, yielding a quantity of de-oiled cakes needing to be handled [24].

De-oiled rapeseed cake (DRC) is the residue produced from rapeseed pressing or chemical leaching to obtain edible oil, where the former residue remains 12–15 wt.% oil component, while the value for the latter is usually less than 1 wt.%. Nowadays, the growing demand for edible oil in China has led to increased production of de-oiled rapeseed cake (DRC), necessitating to actively explore suitable methods for recycling DRC waste rather than utilization as a fertilizer in the soil or as an ingredient in animal feed, the conventional way of treatment. However, achieving high-value valorization of DRC remains challenging. Thus, exploring new approaches to valorize DRC into energy-rich products through thermochemical processes (such as pyrolysis) or its valorization into renewable fuels or commercial chemicals is of significance to realize the effective valorization of renewable wastes. As the residue of the oil pressing process, DRC retains oil components of approximately 12–15 wt.%, which is favorable in the acquisition of oil, as well as in increasing the quality of products obtained, indicating that DRC is naturally suitable for pyrolysis yielding bio-oil (bio-fuel), biochar and gaseous products (CO, CO_2, H_2, light hydrocarbons) or value-added chemicals [25,26]. Recent studies have shown that oil seeds can be converted into value-added products using pyrolysis, such as safflower seed, tamarind seed, and castor seed, with an acceptable yield of bio-oil (44, 45 and 64.4 wt.%) at 400, 500 and 550 °C, respectively, the corresponding investigation indicated that acceptable bio-oil yield could have resulted ranging over 400–600 °C [24,27–29].

This research delves into the pyrolysis of de-oiled rapeseed cake using a fixed-bed laboratory-scale pyrolysis system targeted for bio-oil, bio-char, and bio-gas aiming at

fostering a circular economy and, most importantly, striving for net-zero carbon emissions based on slow pyrolysis technique. Key parameters such as pyrolysis temperature, carrier gas flow rate (N_2), retention time, and volumes of condenser were investigated to obtain bio-oil with high yield and better quality. The analysis and exploration of its characteristics are conducted using spectroscopies and chromatography-related related techniques.

2. Materials and Methods

2.1. Feedstock

De-oiled rapeseed cakes (DRC), which are the solid residues left after the traditional rapeseed pressing process, were procured from Pengzhou County in Sichuan Province, located in the southwest region of the People's Republic of China. These DRC were finely ground and sifted to obtain particles with diameters less than 0.18 mm ($D_p \leq 0.18$ mm) before undergoing lyophilization for further analysis. Various analyses were conducted to assess the proximate, ultimate, and chemical composition of the samples. The essential characteristics of the feedstocks are summarized in Table 1.

Table 1. Main characteristics of DRC.

Proximate Analysis (wt.%)		Ultimate Analysis (wt.%)		Composition Analysis (wt.%)	
VM [a]	71.87	C	46.96	Cellulose	9.89
FC [b]	20.98	H	6.98	Hemicellulose	18.07
Ash	5.69	N	6.67	Lignin	14.32
Moisture	1.46	O [c]	38.36	Protein	34.48
		S	1.03	Extractives	15.13
		H/C	1.77		
		O/C	0.61		
		HHV [d], $MJ \cdot kg^{-1}$	19.62		

[a] VM represents Volatile matter; [b] FC stands for Fixed carbon; [c] calculated by difference; [d] HHV refers to a higher heating value.

Commercially available chemicals, solvents, and reagents were employed as received in the study. The solvents and reagents were purchased from Chengdu Kelong Chemical Co., Ltd., Chengdu, China, while the carrier gas (N_2), with a purity of 99.999%, was provided by the Southwest Institute of Chemical Co., Ltd., Chengdu, China.

2.2. Pyrolysis System and Procedure

The pyrolysis experiments were conducted using a fixed-bed reaction system, illustrated in Figure S1. This system comprised a quartz pyrolizer unit, a heating unit, and a condenser unit (consisting of tandem cooling traps), as previously described in our earlier work [30]. In each trial, an initial purge with N_2 was carried out, followed by placing a 5.0 g sample. The sample was heated from room temperature to the final temperature using a fixed heating rate of 25 $°C \cdot min^{-1}$ under a continuous N_2 flow, as per our prior research findings [31]. The samples were held at the maximum treatment temperature of no more than 2 h, and the resulting solids were referred to as DRCR (de-oiled rapeseed cake residue). The volatile products of the reaction were swept from the reaction zone by a carrier gas of N_2. Gaseous and liquid products were collected based on their condensability. Condensable volatiles were collected through the outer quartz tube and condensers, while non-condensable volatiles were sampled using a gas bag. Investigations of pyrolysis parameters such as reaction temperature, purge gas rates, duration time, and volumes of tandem condensers were conducted in four separate sets.

The first set was to evaluate the effect of reaction temperature from 400 to 800 °C under fixed purge gas (N_2) rates of 50 and 80 $mL \cdot min^{-1}$ for inner and outer tubes, respectively.

To evaluate the effect of purge gas velocity on the products' yield and composition, corresponding experiments were conducted at flow rates of either 30 plus 40, 40 plus 60, 50 plus

80, 60 plus 100, or 70 plus 120 mL·min^{-1} for inner and outer tubes, respectively. In this set, the pyrolysis temperature was taken as 600 °C based on the result of the first set of investigations.

In the third set of investigations, the effect of the volumes of the cooling trap was performed. Corresponding variants for the two tandem condensers were 15 + 15, 15 + 210, and 210 + 210 cm^3, respectively, where pyrolysis temperature was taken as 600 °C, flow rates fixed at 50 + 80 mL·min^{-1} for inner and out quartz tubes, and heating rates was set at 25 °C·min^{-1} with retention time of 0.5 h.

For the fourth set of investigation, retention times ranging from 0 to 2 h were investigated, and corresponding variants were set 0 h, 0.5 h, 1.0 h, 1.5 h, and 2.0 h, respectively, where other pyrolysis parameters were chosen based on single-factor optimization method of 1st to 3rd parameter optimization.

After pyrolysis, the system was cooled under N_2 (10 mL·min^{-1} in two tubes, respectively) to ambient temperature before product recovery. Solids remained, and apparatus before and after pyrolysis were weighted. The liquid yield (Y_{liuqid}) is counted by the mass difference of the outer tube and condensers before and after the reaction, and the gas yield (Y_{gas}) is determined by the overall mass balance. All experimental data reported are mean with triplicate runs with ±0.5% deviation.

Characterization and analysis details are provided in the Supplementary Materials.

3. Results and Discussion

3.1. Properties of Feedstock

As presented in Figure S2, where TGA and DTG curves were given, the thermal degradation behavior of DRC showed three inflection points located at 245, 305, and 359 °C, respectively, representing three maximum weight loss rates over the corresponding temperature regions. The total weight loss of the DRC was 71.18 wt.% over the range from 30 to 800 °C. Similar findings have been observed in our previous research on pyrolysis of *pubescens* [32]. It could be observed that with increasing temperature from 400 to 800 °C, the conversion rates augmented continuously, indicating the enhanced weight loss with augmented temperature, whereas there was no obvious degradation above 600 °C, which was similar to the findings reported by Chen et al. using oil plant wastes as starting material [33]. Considering the energy input and efficiency of feedstock valorization, investigations on pyrolysis temperature were selected as 400, 500, 600, 700, and 800 °C. Subsequently, the related effect of pyrolysis temperatures on the distribution of its products, characteristics of bio-chars, and composition of bio-gas obtained was analyzed and discussed in detail as an example of pyrolysis parameters optimization. The details of the optimization of other parameters were provided in Supplementary Materials.

Proximate, ultimate, and components analysis of DRC are presented in Table 1. Compared to lignocellulosic biomass, DRC contains more protein and extractives, which might be favorable for obtaining high-quality bio-oil.

3.2. Effect of Pyrolysis Temperatures on Products Distribution

The pyrolysis temperature is a crucial factor that significantly affects the resulting products obtained from the process, which has been investigated in the pyrolysis of lignocellulosic biomass, sludges, high/low-density polyethylene, etc. [34–36]. Thus, the effect of the final heating temperature on the pyrolysis of DRC was carried out as well. Product distribution under 5 final temperatures with fixed purge gas rates (50 and 80 mL·min^{-1} for inner and outer tubes, respectively.), heating rates (25 °C·min^{-1}) chosen according to our previous work [31] was presented in Figure 1 and Table S1. With an increase in temperature, $Y_{liquids}$ augmented initially from 40.4 to 51.6 wt.% in the temperature range over 400–600 °C, after that declined till 45.4 wt.% in the range over 600–800 °C. The corresponding char yield decreased from 41.8 to 31.4 wt.% and then declined to 28.8 wt.%, while the gas yield varied slightly, from 17.8 to 17.0 wt.%, and then augmented to 25.8 wt.%. The decrease in liquids above 600 °C could be attributed to the enhanced pyrolysis of volatiles from intermediate compounds. Char yield decreased with increasing temperatures owing to carbon material decomposition

promoted at higher temperatures. The maximum liquid yield (51.6 wt.%) was obtained at 600, indicating that 600 °C was the optimal value for DRC valorization and was selected as the optimum value in further investigations. It could be observed that the yield of pyrolysis liquid is acceptable, ranging from 40.4 to 51.6 wt.%, higher than that of lignocellulose (37.3 to 40.3 wt.% in the range of 400–600 °C) [37], yielding less solid char but more liquid products. Thus, the pyrolysis of DRC appears to be a promising alternative for the production of biofuel (bio-oil) to other biomass such as woody and herbaceous biomass.

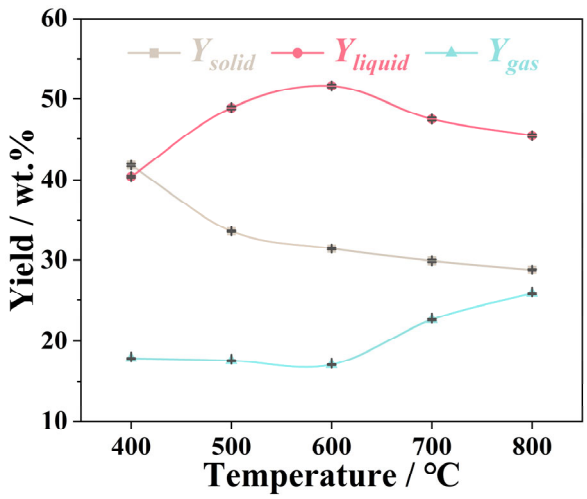

Figure 1. Product distribution at 5 final pyrolysis temperatures (400, 500, 600, 700, 800 °C), 50 and 80 mL·min^{-1} for inner and outer tubes, retention time of 0.5 h, volumes of condensers with 210 + 210 cm^3.

3.3. Effect of Pyrolysis Temperatures on Characteristics of Bio-Chars

In this investigation, vital pyrolysis conditions and pyrolysis temperatures were investigated on the properties of bio-chars obtained, as had been investigated by other researchers using different feedstocks [38,39]. Biochar modification scenarios under H_2O_2 oxidation from different feedstocks and pyrolysis conditions were investigated by Ghorbani et al., achieving enhanced specific surface area and porosity in all oxidized bio-chars [40]. Moreover, biochar production from carbonization of biomass or de-oiled wastes on a pilot scale or above was of engineering and energetically interest owing to its industrially viable and ease to operate, as liquids could be burnt to supply heat for carbonization but with difficulty in swift purge and cool of volatiles generated in reaction zone, which was defined by the fixation of effective carbon into solid chars, whereas pyrolysis for liquids aiming at elevating the effective carbon content for more condensable volatiles acquisition [41–43]. In this research, the yield of biochar declined from 41.8 to 21.8 wt.% by an augmented reaction temperature ranging from 400 to 800 °C (seen in Table S1). At 400 °C, the pyrolysis process was presumed to be incomplete, leading to unreacted DRC retained within the biochar, which elucidated the bio-char's higher heating value (HHV) of 29.03 MJ·kg^{-1} at this temperature. Subsequently, augmenting temperature to 500 °C reduced the proportion of the bio-char component, consequently leading to a slight increase in HHV to 29.56 MJ·kg^{-1}, with further increase in pyrolysis temperature, the corresponding value increased up to 30.10, 30.10, and 30.14 MJ·kg^{-1} at 600, 700 and 800 °C, respectively. These HHV values are higher than that of the DRC at 19.62 MJ·kg^{-1}, as indicated in Table S2. Corresponding values of H/C and O/C molar ratios of DRC and chars are shown in Figure 2. With the increase in pyrolysis temperature, H/C and O/C values decreased from 1.77 to 0.52 and 0.61 to 0.16, which was enhanced in comparison with that of lignocellulosic biomass (*pubescens*) [30], where corresponding values varied from 1.55 to 0.66, and 0.63 to 0.22, respectively, indicating the coalification of chars enhanced by higher temperatures. Consequently, the solid product, or biochar, could be effectively utilized as a solid fuel source or precursor to functional carbons, as previously investigated by Wang et al. [30].

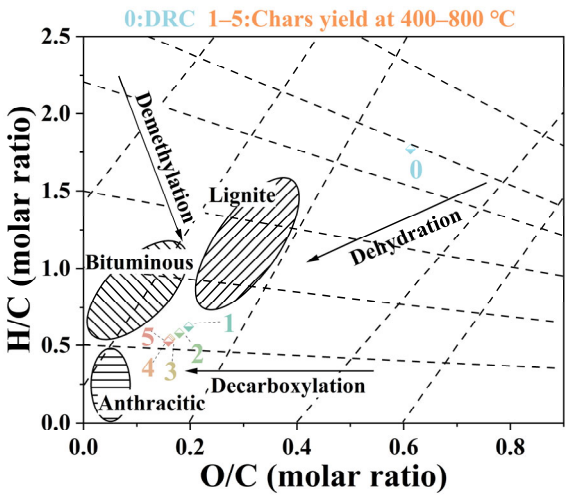

Figure 2. Van Krevelen diagram of DRC and chars investigated by different temperatures.

3.4. Effect of Pyrolysis Temperatures on Composition of Gaseous Products Obtained

With the increase of temperatures ranging from 400 to 800 °C, the yield of gaseous products increased from 17.8 to 25.8 wt.%, higher than the value (12.48 to 21.11% and 12.10–16.99% in the range from 600 to 800 °C) obtained through pyrolysis of two biomass feedstock reported by Wu et al. [44]. Detailed composition of gases released and corresponding lower heating value (LHV) are presented in Table S3, Figure 3 and Figure S3. The gaseous products were mainly composed of CO_2, CO, C_1 and C_2 hydrocarbons, and H_2, where CO_2 and CO have resulted from oxygenated compounds fatty acids, holocellulose, and lignin from DRC. Corresponding LHVs were calculated based on Equation (S2) seen in Supplementary Materials. As could be observed, LHV increased from 5.92 MJ·Nm^{-3} at 400 °C to 7.63 MJ·Nm^{-3} at 600 °C and then declined to 7.50 and 7.40 MJ·Nm^{-3} at 700 and 800 °C, respectively. Small amounts of C_1, C_2 hydrocarbons, and H_2 could be yielded, indicating that strengthened reactions took place during pyrolysis at higher temperatures. The acquisition of H_2 was poor, which was similar to research findings reported by Uddin et al., where the yield of hydrogen gas varies from various feedstocks during pyrolysis, influenced by secondary reactions such as excessive thermal cracking caused by insufficient purging [45]. Moreover, in the case of a specific feedstock, the volatile matter remains constant, and a high yield of liquids corresponds to a low yield of gaseous products. Consequently, the specific composition of the gaseous products aligns with a lower yield.

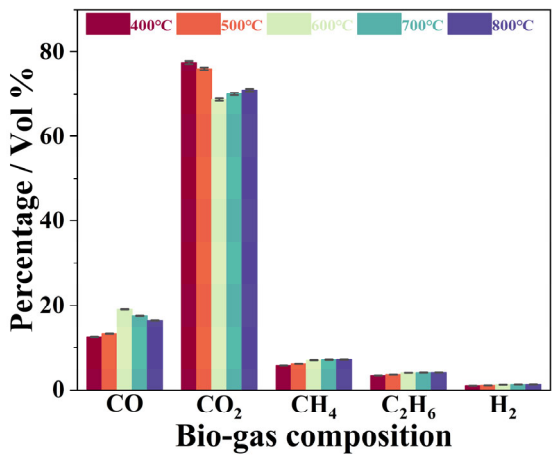

Figure 3. Gaseous product composition at different temperatures.

3.5. Optimization of Pyrolysis Parameters

The optimization of several key pyrolysis parameters, including carrier gas rates, retention time at peak temperature, and volume of tandem condensers, evaluated by maximum bio-oil yield, was carried out as described above, and the results were shown in Figure 4a–c. While researchers had individually investigated each of the aforementioned parameters, there is a limited number of research findings that comprehensively explore the combined impact of these parameters on the product results [46,47]. Herein, an integrated influence of key pyrolysis parameters on the yield of liquid products obtained was performed.

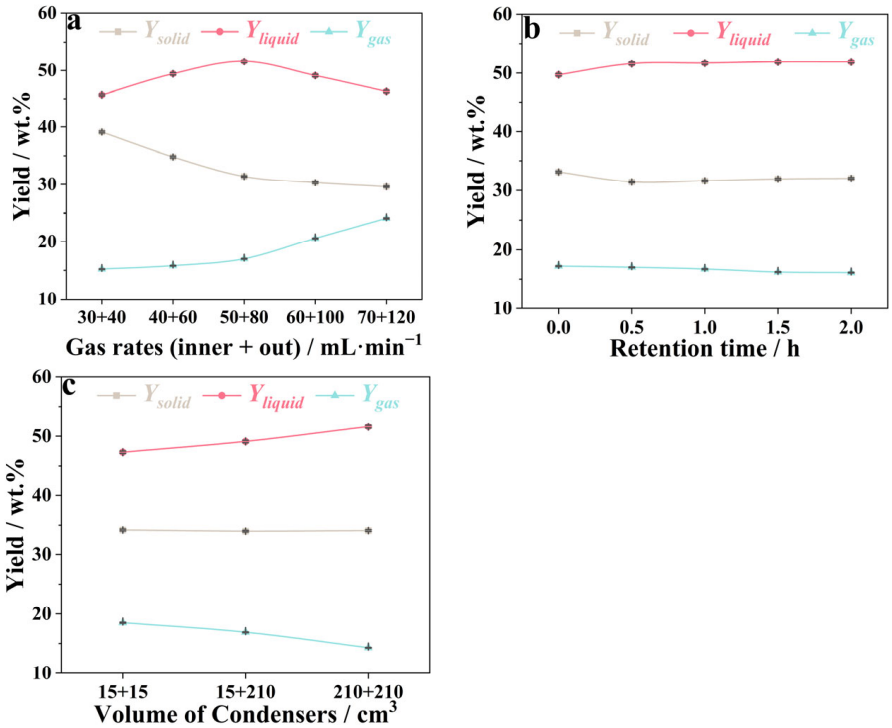

Figure 4. (**a**) Product distribution under different flow gas rates (30 + 40—70 + 120 mL·min^{-1}, pyrolysis temperature at 600 °C, retention time of 0.5 h, volumes of condensers with 210 + 210 cm^3); (**b**) Product distribution under different retention time (0–2 h, pyrolysis temperature at 600 °C, 50 and 80 mL·min^{-1} for inner and outer tubes, volumes of condensers 210 + 210 cm^3); (**c**) Product distribution under different volume of condensers ((15 + 15) –(210 + 210) cm^3, pyrolysis temperature at 600 °C, 50 and 80 mL·min^{-1} for inner and outer tubes, retention time of 0.5 h).

For carrier gas rate optimization, as shown in Figure 4a and Table S4, the corresponding liquid yield was 49.4 and 50.3 wt.% for 30 plus 40 and 40 plus 60 mL·min^{-1}, respectively. The maximum liquid yield (51.6 wt.%) could be obtained with an increase in the gas rates to 50 plus 80 mL·min^{-1}, which was higher than that of pyrolysis of Cotton seed with MgO catalyst, where the corresponding value was 48.3 wt.% with flow gas rates of 200 mL·min^{-1} [48]. With further augment of the flow gas rates to 60 plus 100 and 70 plus 120 mL·min^{-1}, the corresponding yield declined to 50.7 and 49.8 wt.%, respectively. Thus, 50 + 80 mL·min^{-1} was chosen as the optimal gas rate.

Regarding the duration time optimization, as shown in Figure 4b and Table S5, the yield of pyrolytic liquid increased by 1.9 wt.% when the retention time was prolonged to 0.5 h from 0 h, while little variation could be observed on liquid yield with further increase in retention time, which was higher than that of the value obtained from pyrolysis of neem press seed cake, as there was no significant influence on the liquid yield caused by retention time using RSM modeling and analyzing [46]. Thus, 0.5 h was chosen as the optimized duration time.

For the optimization of volumes of tandem condensers, as shown in Figure 4c and Table S6, with the increase of the volume of tandem condensers, the yield of pyrolytic liquid increased by 1.8 and 4.3 wt.%, respectively, owing to the effective condensation of volatiles rather than insufficient cooling, indicating that augment the volume of condensers could enhance the yield of bio-liquids in a certain degree. The influence of pyrolytic volatile condensation under different temperatures has been investigated using various feedstocks, while research related to the effect of volumes of tandem condensers on the variation of liquid yield was limited [49,50].

Detailed discussions on the composition of bio-oils obtained based on parameter optimization are presented in Supplementary Materials to avoid tedious repetition.

3.6. Characteristic of Bio-Oil Obtained from DRC Pyrolysis with Optimized Parameters

The bio-oil obtained under optimized parameters was analyzed via several techniques and presented in Table 2. Corresponding characteristics of pyrolysis oil from lignocellulosic biomass, bio-diesel, and petroleum diesel were listed for comparison. The influence of related parameters such as purge gas rates, retention time, and condensation duration on product distribution and variation of bio-oil fractions has been investigated thoroughly as well, the details of which were given in Supplementary Materials to avoid tedious repetition (seen as Tables S4–S10).

Table 2. Characteristic of the pyrolysis bio-oil, bio-diesel, and petroleum diesel.

Ultimate Analysis/wt.%	Category			
	Pyrolysis Bio-Oil of DRC	**Pyrolysis Bio-Oil of Lignocellulosic Biomass [37,51]**	**Bio-Diesel [52–55]**	**Petroleum Diesel [52,53]**
C	67.41	53.56–61.19	59.94–78.10	86.58
H	8.64	4.91–7.98	11.00–12.40	13.29
N	8.99	0.53–2.48	0.07–0.50	0.01
S	0.55	-	0.06–0.31	<0.11
O [a]	14.41	25.39–36.39	9.23–23.87	0.01
H/C atomic ratio	1.53	0.96–1.77	1.89–2.18	1.83
O/C atomic ratio	0.16	0.36–0.50	0.09–0.30	<0.001
Moisture/wt.%	4.87	>10	<0.05	<0.03
Viscosity (40 °C, $mm^2 \cdot s^{-1}$)	413.22	-	5.66–5.82	2–4.5
TAN (mg KOH/g)	44.51	-	<0.5	<0.5
Density (g/mL)	1.21	-	>0.86	0.86–0.90
Surface tension (25 °C $mN \cdot m^{-1}$)	24.10	-	-	-
HHV ($MJ \cdot kg^{-1}$)	32.82	21.37–26.96	20.80–41	>43

[a] calculated by difference.

The carbon content in the bio-oil of DRC was 67.41 wt.%, which was in the variation range of bio-diesel, higher than that of bio-oil from lignocellulose, but lower than that of petroleum diesel. The corresponding value of hydrogen in bio-oil was 8.64 wt.%, much higher than that of pyrolysis oil from lignocellulose but lower than that of both of the other types of diesels. HHV of the bio-oil was 32.82 $MJ \cdot kg^{-1}$, lower than both the high limit of bio-diesel and petroleum diesel, while higher than that of lignocellulosic bio-oil, but in the HHV value range of the bio-diesel, that is, it is close to fuel of transportation grade. The determined moisture was 4.87 wt.%, much lower than pyrolysis bio-oils from lignocellulosic biomass such as sugarcane, *pubescens*, and camellia oleifera shell, usually ranging from 10 to 30 wt.%, but higher than that of bio-diesel and petroleum diesel (lower than 0.05 and 0.03 wt.%, respectively).

The viscosity of the bio-oil was 413.22 $mm^2 \cdot s^{-1}$, hundreds of times higher than that of bio-diesel and petroleum diesel, which was above the range of diesel standard. The density of the bio-oil remained at 1.21 $g \cdot mL^{-1}$, close to that of bio-diesel and diesel (>0.86 and 0.86–0.90 g/mL, respectively). As for the surface tension, a key characteristic of biofuel facilitating the emulsion formation, the corresponding value was comparatively low, which was 24.10 $mN \cdot m^{-1}$, lower than that of petroleum diesel (26.20). The acidity of bio-oil (determined by TAN) was 44.51 mg KOH/g, significantly higher than that of bio-diesel and diesel (<0.5 mg KOH/g), where the lower value is attributed to the existence of more acids, which was in accordance with our previous research and the composition analysis through GC-MS.

FT-IR was introduced to identify the functional groups that existed in the bio-oil obtained at optimized values, and the spectra was presented in Figure 5 (2000–500 cm^{-1}) and Figure S4 (4000–500 cm^{-1}). Characteristic absorbances of the bio-oil were assigned according to the literature [56–60]. The outcomes highlighted the existence of organic compounds within the sample.

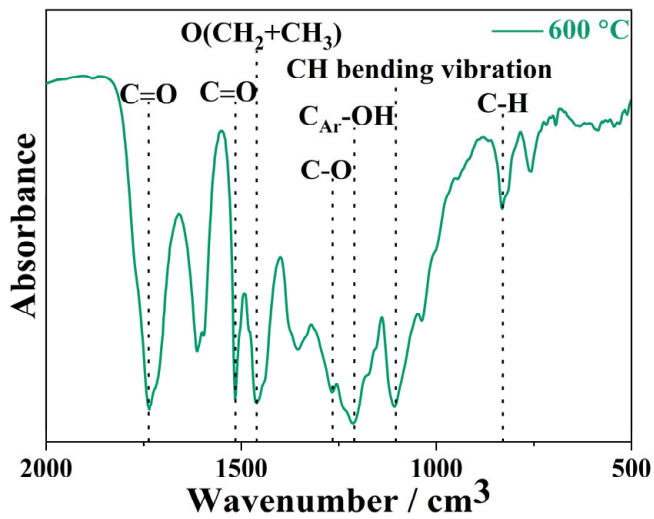

Figure 5. FT-IR spectra of bio-oil obtained at optimized values ranging from 2000–500 cm^{-1}.

As shown in Figure S4, the band above 3440 cm^{-1}, ascribed to –OH stretching vibrations, was observed, and this observation could be attributed to alcohols, acids, phenols, and water. Band between 2732–3064 cm^{-1} was assigned to C–H stretching vibration of methyl and methylene groups, which underscores the significance of saturated aliphatic hydrocarbons in the composition of bio-oil. No obvious variations could be observed in the range from 4000 to 2000 cm^{-1} in comparison with bio-oil obtained at different temperatures. The bands at 1738 and 1514 cm^{-1} were assigned to the presence of C=O, as well as carbonyl-containing compounds, which indicated the existence of featured species with C=O group such as aldehydes, ketones, carboxylic acids, and ester compounds, and were further enhanced with higher pyrolysis temperature than 400 °C. The band at 1456 cm^{-1} aligned with the asymmetric vibrations of $–CH_2–$ and $–CH_3$ functional groups, while the band at 1278 cm^{-1} was associated with the presence of C–O groups, possibly arising from ester and alcohol structures. Moreover, bands at 1456 and 1210 cm^{-1} were ascribed to the vibration of the aromatic ring skeleton and –OH stretching attached to a benzene ring, indicating the presence of an aromatic ring. The band at 1112 cm^{-1} was assigned to the bending vibration of C–H, indicative of aromatic compounds. Notably, the band at 829 cm^{-1} was assigned to C–H out of plane deformation of G and S units of lignin, inductive of characteristic aromatic vibrations, specifically associated with the vibration of lignin units [61]. The FT-IR results provide a glimpse into the intricate composition of the obtained bio-oil.

GC-MS was also introduced to further elucidate the composition of the bio-oil obtained from pyrolysis of DRC, where compounds were classified with the declined peak area (seen in Table S11). To achieve this, the bio-oil sample was intentionally diluted using tetrahydrofuran (THF). The resulting chromatographic diagram revealed an array of more than 100 peaks, and the constituents were meticulously identified by referencing the NIST library. Given the intricate nature of the bio-liquid (bio-oil), the chromatographical analysis revealed a complex amalgamation of compounds stemming from the decomposition of diverse components, including cellulose, hemicellulose, lignin, protein, and extractives. While the experimental configurations exhibited similar compositions, variations in component reports were observed. As shown in Figure 6, groups were classified as Acids, Hydrocarbons, Phenols, Esters, Alcohols, Ketones, N-compounds, Levoglucosenone and Monoglycerides. As investigated by David et al. [62], bio-oils were found to have consisted of alkanes, alkenes, alkadienes, aromatic hydrocarbons, and fatty acids as a result of the primary and secondary reactions occurring during the pyrolysis.

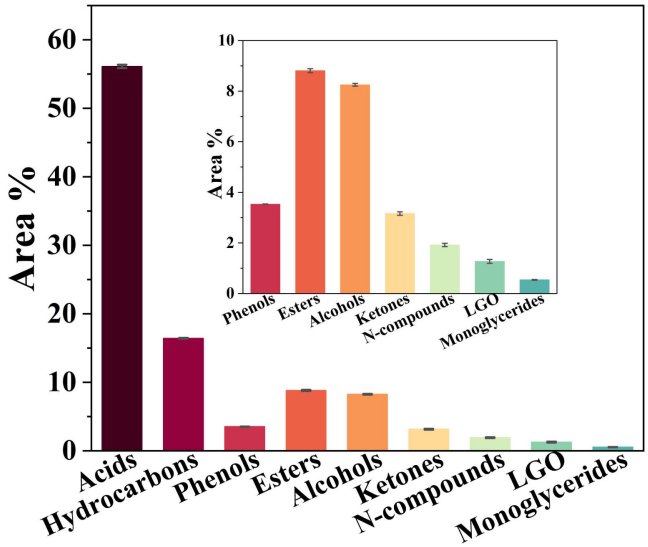

Figure 6. Qualitatively identify the composition of bio-oils under optimized parameters.

As could be observed, the yield of acids (such as Acetic acid, n-Hexadecanoic acid, Octadecanoic acid, Tetradecanoic acid, and Oleic acid) was more than 56%, most importantly, the yield of hydrocarbons, indicator of commercial fuels (such as Heptadecane, Pentadecane and 2,6,6-Trimethyl-bicyclo[3.1.1]heptane) was 16.41%. For other kinds of compounds, the percentage of each was lower than 10%. Among them, esters and alcohols were more than 8%, followed by phenols and ketones, with corresponding values of 3.53 and 3.16%, respectively. The other three species took the other yield of 3.73%, where minor constituents, such as N-compounds, have been noted by our previous research, underlining the precursor role of proteins and the origin of phenols from lignin fragments, as well as protein [63]. In fact, the conversion of acids into hydrocarbons has been widely studied [64,65], providing clues to the upgrading of the pyrolysis bio-oil. That is, the downstream processing of pyrolysis bio-oil from DRC is promising compared to crude bio-liquids from the pyrolysis of lignocellulosic biomass containing many kinds of oligomers [31].

By comparing the characteristic of bio-oil obtained based on the optimized parameter with the pyrolysis bio-oil from lignocellulosic biomass, bio-diesel, and commercial diesel oil, as shown in Table 2, it was found that the H/C and O/C molar ratio and the density are acceptable in comparison with petroleum diesel, but with lower HHV and poor characteristics such as poor carbon and hydrogen content, higher TAN, viscosity and moisture. Its fuel characteristics were comparable to that of bio-diesel, such as similar elemental composition and density, as well as HHV, but with poor viscosity and TAN, as well as higher moisture. Moreover, the characteristics of bio-oil from DRC are superior to those of lignocellulosic

biomass in terms of various properties such as H/C and O/C molar ratio, HHV value, and moisture content. In comparison with the caloric value of commercial diesel oil, as well as the promising bio-diesel, bio-oil from pyrolysis of DRC seemed to be comparable to the bio-diesel mentioned [66], even though with poor characteristics of HHV, high content of moisture, and TAN, which needs further downstream upgrading. It was concluded that the bio-oil obtained through pyrolysis of DRC was superior to that derived from lignocellulosic biomass and was significantly superior to the latter for utilization in industrial boilers or agricultural engines. Moreover, downstream upgrading of the bio-oil is indispensable for valorization of the bio-oil into the transportation fuels, such as catalytic conversion of acids (such as n-hexadecanoic acid, octadecanoic acid, tetradecanoic acid, and oleic acid, etc.) into hydrocarbons via decarboxylation of long-chain acids, as well as hydrodeoxygenation of the bio-oil with better caloric value [67–70].

4. Conclusions

De-oiled rapeseed cake (DRC), a byproduct of agricultural rapeseed pressing, emerges as a promising source for liquid fuel production with acceptable quality via slow pyrolysis. Optimal bio-oil yields of 51.6 wt.% are attainable under optimized conditions with corresponding bio-oil's higher heating value (HHV) of 32.82 MJ·kg^{-1}, outperforming that of lignocellulosic biomass, comparable to biodiesel, but being less than petroleum diesel, which was appliable for scale-up application for energy production from effective waste utilization. With additional processing, such as decarboxylation and hydrodeoxygenation, this bio-oil shows promise for use in transportation fuels. In conclusion, DRC-derived bio-oil aligns closely with transportation fuel standards, and the resultant pyrolyzed char has potential as either a solid fuel or a precursor for functional carbon materials in various applications.

Supplementary Materials: The following supporting information can be downloaded at https://www.mdpi.com/article/10.3390/en17030612/s1, Figure S1: Frame diagram of pyrolysis process, Figure S2: The TGA and DTG curves of de-oiled rapeseed cake, Figure S3: LHV of gaseous products at different temperatures (calculated according to [71]), Figure S4: FT-IR spectra of bio-oils from different pyrolysis temperatures. Left panel shows the whole spectra ranging from 4000–500 cm^{-1}, right panel indicates the specific spectra ranging from 2000–500 cm^{-1}; Table S1: Products Distribution via different pyrolysis temperatures, Table S2: Ultimate, Proximate and HHV of DRC and bio-chars investigated by temperatures (calculated according to [72–74] respectively), Table S3: Composition of gaseous products obtained at different temperature, Table S4: Products Distribution via different flow gas rates, Table S5: Products Distribution via different flow retention time, Table S6: Products Distribution via different volume of condensers, Table S7: Physical chemical characteristics of the bio-oils obtained from DRC pyrolysis temperature at 5 intervals (400–800 °C, 50 and 80 mL·min^{-1} for inner and outer tubes, retention time of 0.5 h, volumes of condensers with 210 + 210 cm^3), Table S8: Physical chemical characteristics of the bio-oils obtained from DRC pyrolysis at 5 flow gas rates (30 + 40 − 70 + 120 mL·min^{-1}, 50 plus 80 mL·min^{-1} for inner and outer tubes, retention time of 0.5 h, volumes of condensers with 210 + 210 cm^3), Table S9: Physical chemical characteristics of the bio-oils obtained from DRC pyrolysis at 5 retention times (0–2 h with step of 0.5 h, pyrolysis temperature at 600 °C, 50 plus 80 mL·min^{-1} for inner and outer tubes, respectively, retention time at 0.5 h, volumes of condensers with 210 + 210 cm^3), Table S10: Physical chemical characteristics of the bio-oils obtained from DRC pyrolysis at 3 tandem condensers (15 + 15) − (210 + 210) cm^3, pyrolysis temperature at 600 °C, retention time of 0.5 h, 50 plus 80 mL·min^{-1} for inner and outer tubes, respectively, Table S11: The relative content of compounds in the bio-oil under 5 pyrolysis temperatures.

Author Contributions: Y.W.: Conceptualization, Methodology, Validation, Formal analysis, Resources, Data curation, Software, Writing Original Manuscript, Visualization. Y.Z.: Software, Visualization, Analysis. C.H.: Conceptualization, Methodology, Writing—reviewing & editing, Supervision, Project administration, Funding acquisition. All authors have read and agreed to the published version of the manuscript.

Funding: This work was financially supported by the National Key R&D Program of China (2018YFB1501404, Ministry of Science and Technology of the People's Republic of China).

Data Availability Statement: Data will be available when requested.

Acknowledgments: The characterization from the Analytical and Testing Center of Sichuan University, State Key Laboratory of Polymer Materials Engineering (Sichuan University), and Analysis and Test Center of the Chengdu Branch of the Chinese Academy of Sciences were greatly appreciated.

Conflicts of Interest: The authors declare that they have no known competing financial interests or personal relationships that could have appeared to influence the work reported in this article.

References

1. Chen, J.M. Carbon neutrality: Toward a sustainable future. *Innovation* **2021**, *2*, 100127. [CrossRef]
2. Queneau, Y.; Han, B. Biomass: Renewable carbon resource for chemical and energy industry. *Innovation* **2021**, *3*, 100184. [CrossRef]
3. Wang, F.; Harindintwali, J.D.; Yuan, Z.; Wang, M.; Wang, F.; Li, S.; Yin, Z.; Huang, L.; Fu, Y.; Li, L.; et al. Technologies and perspectives for achieving carbon neutrality. *Innovation* **2021**, *2*, 100180. [CrossRef]
4. Yang, Q.; Zhou, H.; Bartocci, P.; Fantozzi, F.; Masek, O.; Agblevor, F.A.; Wei, Z.; Yang, H.; Chen, H.; Lu, X.; et al. Prospective contributions of biomass pyrolysis to China's 2050 carbon reduction and renewable energy goals. *Nat. Commun.* **2021**, *12*, 1698. [CrossRef]
5. Obersteiner, M.; Bednar, J.; Wagner, F.; Gasser, T.; Ciais, P.; Forsell, N.; Frank, S.; Havlik, P.; Valin, H.; Janssens, I.A.; et al. How to spend a dwindling greenhouse gas budget. *Nat. Clim. Change* **2018**, *8*, 7–10. [CrossRef]
6. Anderson, K.; Peters, G. The trouble with negative emissions. *Science* **2016**, *354*, 182–183. [CrossRef]
7. Liu, W.-J.; Li, W.-W.; Jiang, H.; Yu, H.-Q. Fates of Chemical Elements in Biomass during Its Pyrolysis. *Chem. Rev.* **2017**, *117*, 6367–6398. [CrossRef]
8. Liu, C.; Wang, H.; Karim, A.M.; Sun, J.; Wang, Y. Catalytic fast pyrolysis of lignocellulosic biomass. *Chem. Soc. Rev.* **2014**, *43*, 7594–7623. [CrossRef]
9. Zhang, S.; Jiang, S.-F.; Huang, B.-C.; Shen, X.-C.; Chen, W.-J.; Zhou, T.-P.; Cheng, H.-Y.; Cheng, B.-H.; Wu, C.-Z.; Li, W.-W.; et al. Sustainable production of value-added carbon nanomaterials from biomass pyrolysis. *Nat. Sustain.* **2020**, *3*, 753–760. [CrossRef]
10. Vispute, T.P.; Zhang, H.; Sanna, A.; Xiao, R.; Huber, G.W. Renewable Chemical Commodity Feedstocks from Integrated Catalytic Processing of Pyrolysis Oils. *Science* **2010**, *330*, 1222–1227. [CrossRef]
11. Cheng, B.H.; Huang, B.C.; Zhang, R.; Chen, Y.L.; Jiang, S.F.; Lu, Y.; Zhang, X.S.; Jiang, H.; Yu, H.Q. Bio-coal: A renewable and massively producible fuel from lignocellulosic biomass. *Sci. Adv.* **2020**, *6*, 8. [CrossRef]
12. Chen, Y.; Yang, H.; Yang, Q.; Hao, H.; Zhu, B.; Chen, H. Torrefaction of agriculture straws and its application on biomass pyrolysis poly-generation. *Bioresour. Technol.* **2014**, *156*, 70–77. [CrossRef]
13. Zhang, X.; Che, Q.; Cui, X.; Wei, Z.; Zhang, X.; Chen, Y.; Wang, X.; Chen, H. Application of biomass pyrolytic polygeneration by a moving bed: Characteristics of products and energy efficiency analysis. *Bioresour. Technol.* **2018**, *254*, 130–138. [CrossRef]
14. Yang, H.; Liu, B.; Chen, Y.; Chen, W.; Yang, Q.; Chen, H. Application of biomass pyrolytic polygeneration technology using retort reactors. *Bioresour. Technol.* **2016**, *200*, 64–71. [CrossRef]
15. Brigljević, B.; Liu, J.J.; Lim, H. Comprehensive feasibility assessment of a poly-generation process integrating fast pyrolysis of S. japonica and the Rankine cycle. *Appl. Energ.* **2019**, *254*, 113704. [CrossRef]
16. Lei, Q.; Zhang, S.; Li, Y.; Ding, X.; Wang, Y.; Zheng, L.; Wu, L. Design and optimization of poly-generation system for municipal solid waste disposal. *J. Clean. Prod.* **2022**, *370*, 133611. [CrossRef]
17. Cong, H.; Meng, H.; Mašek, O.; Yao, Z.; Li, L.; Yu, B.; Qin, C.; Zhao, L. Comprehensive analysis of industrial-scale heating plants based on different biomass slow pyrolysis technologies: Product property, energy balance, and ecological impact. *Clean. Eng. Technol.* **2022**, *6*, 100391. [CrossRef]
18. Lehto, J.; Oasmaa, A.; Solantausta, Y.; Kytö, M.; Chiaramonti, D. Review of fuel oil quality and combustion of fast pyrolysis bio-oils from lignocellulosic biomass. *Appl. Energ.* **2014**, *116*, 178–190. [CrossRef]
19. Stas, M.; Kubicka, D.; Chudoba, J.; Pospísil, M. Overview of Applications of Pyrolysis Bio-oil. *Chem. Listy* **2015**, *109*, 499–506.
20. Mohan, D.; Pittman, C.U.; Steele, P.H. Pyrolysis of wood/biomass for bio-oil: A critical review. *Energ. Fuel* **2006**, *20*, 848–889. [CrossRef]
21. Trinh, T.N.; Jensen, P.A.; Dam-Johansen, K.; Knudsen, N.O.; Sorensen, H.R.; Hvilsted, S. Comparison of Lignin, Macroalgae, Wood, and Straw Fast Pyrolysis. *Energ. Fuel* **2013**, *27*, 1399–1409. [CrossRef]
22. Miao, X.L.; Wu, Q.Y.; Yang, C.Y. Fast pyrolysis of microalgae to produce renewable fuels. *J. Anal. Appl. Pyrolysis* **2004**, *71*, 855–863. [CrossRef]
23. Sun, Y.F.; Li, C.; Zhang, S.; Li, Q.L.; Gholizadeh, M.; Wang, Y.; Hu, S.; Xiang, J.; Hu, X. Pyrolysis of soybean residue: Understanding characteristics of the products. *Renew. Energy* **2021**, *174*, 487–500. [CrossRef]
24. Rajpoot, L.; Tagade, A.; Deshpande, G.; Verma, K.; Geed, S.R.; Patle, D.S.; Sawarkar, A.N. An overview of pyrolysis of de-oiled cakes for the production of biochar, bio-oil, and pyro-gas: Current status, challenges, and future perspective. *Bioresour. Technol. Rep.* **2022**, *19*, 101205. [CrossRef]
25. Ucar, S.; Ozkan, A.R. Characterization of products from the pyrolysis of rapeseed oil cake. *Bioresour. Technol.* **2008**, *99*, 8771–8776. [CrossRef]

26. Ozcimen, D.; Karaosmanoglu, F. Production and characterization of bio-oil and biochar from rapeseed cake. *Renew. Energ.* **2004**, *29*, 779–787. [CrossRef]
27. Kader, M.A.; Islam, M.R.; Parveen, M.; Haniu, H.; Takai, K. Pyrolysis decomposition of tamarind seed for alternative fuel. *Bioresour. Technol.* **2013**, *149*, 1–7. [CrossRef]
28. Sensoz, S.; Angin, D. Pyrolysis of safflower (*Charthamus tinctorius* L.) seed press cake: Part 1. The effects of pyrolysis parameters on the product yields. *Bioresour. Technol.* **2008**, *99*, 5492–5497. [CrossRef]
29. Singh, R.K.; Shadangi, K.P. Liquid fuel from castor seeds by pyrolysis. *Fuel* **2011**, *90*, 2538–2544. [CrossRef]
30. Wang, Y.; Wurzer, C.; Wang, W.; Liu, Y.; Liu, L.; Lv, X.; Mašek, O.; Hu, C. Enhancing the production of small molecular products from pubescens via stepwise pyrolysis process. *J. Anal. Appl. Pyrolysis* **2022**, *168*, 105708. [CrossRef]
31. Li, Q.X.; Fu, X.; Li, J.D.; Wang, Y.; Lv, X.Y.; Hu, C.W. Effect of Heating Rate on Yields and Distribution of Oil Products from the Pyrolysis of Pubescen. *Energy Technol.* **2018**, *6*, 366–378. [CrossRef]
32. Lv, X.; Jiang, Z.; Li, J.; Wang, Y.; Tong, D.; Hu, C. Low-Temperature Torrefaction of Phyllostachys heterocycla cv. pubescens: Effect of Two Torrefaction Procedures on the Composition of Bio-Oil Obtained. *ACS Sustain. Chem. Eng.* **2017**, *5*, 4869–4878. [CrossRef]
33. Chen, J.; Fan, X.; Jiang, B.; Mu, L.; Yao, P.; Yin, H.; Song, X. Pyrolysis of oil-plant wastes in a TGA and a fixed-bed reactor: Thermochemical behaviors, kinetics, and products characterization. *Bioresour. Technol.* **2015**, *192*, 592–602. [CrossRef]
34. Moško, J.; Pohořelý, M.; Skoblia, S.; Beňo, Z.; Jeremiáš, M. Detailed Analysis of Sewage Sludge Pyrolysis Gas: Effect of Pyrolysis Temperature. *Energies* **2020**, *13*, 4087. [CrossRef]
35. Santos, J.; Ouadi, M.; Jahangiri, H.; Hornung, A. Valorisation of lignocellulosic biomass investigating different pyrolysis temperatures. *J. Energy Inst.* **2020**, *93*, 1960–1969. [CrossRef]
36. Sogancioglu, M.; Yel, E.; Ahmetli, G. Pyrolysis of waste high density polyethylene (HDPE) and low density polyethylene (LDPE) plastics and production of epoxy composites with their pyrolysis chars. *J. Clean. Prod.* **2017**, *165*, 369–381. [CrossRef]
37. Dai, L.; Wang, Y.; Liu, Y.; Ruan, R.; Yu, Z.; Jiang, L. Comparative study on characteristics of the bio-oil from microwave-assisted pyrolysis of lignocellulose and triacylglycerol. *Sci. Total Environ.* **2019**, *659*, 95–100. [CrossRef]
38. Zhang, X.; Zhang, P.; Yuan, X.; Li, Y.; Han, L. Effect of pyrolysis temperature and correlation analysis on the yield and physicochemical properties of crop residue biochar. *Bioresour. Technol.* **2020**, *296*, 122318. [CrossRef]
39. Ortiz, L.R.; Torres, E.; Zalazar, D.; Zhang, H.; Rodriguez, R.; Mazza, G. Influence of pyrolysis temperature and bio-waste composition on biochar characteristics. *Renew. Energ.* **2020**, *155*, 837–847. [CrossRef]
40. Ghorbani, M.; Konvalina, P.; Neugschwandtner, R.W.; Soja, G.; Bárta, J.; Chen, W.-H.; Amirahmadi, E. How do different feedstocks and pyrolysis conditions effectively change biochar modification scenarios? A critical analysis of engineered biochars under H_2O_2 oxidation. *Energ. Convers. Manag.* **2024**, *300*, 117924. [CrossRef]
41. Gonzalez, J.M.; Boddu, V.M.; Jackson, M.A.; Moser, B.; Ray, P. Pyrolysis of creosote -treated railroad ties to recover creosote and produce biochar. *J. Anal. Appl. Pyrolysis* **2020**, *149*, 104826. [CrossRef]
42. Kazimierski, P.; Hercel, P.; Januszewicz, K.; Kardas, D. Pre-Treatment of Furniture Waste for Smokeless Charcoal Production. *Materials* **2020**, *13*, 3188. [CrossRef]
43. Bartoli, M.; Rosi, L.; Giovannelli, A.; Frediani, P.; Frediani, M. Characterization of bio-oil and bio-char produced by low-temperature microwave-assisted pyrolysis of olive pruning residue using various absorbers. *Waste Manag. Res.* **2020**, *38*, 213–225. [CrossRef]
44. Wu, Z.; Zhang, B.; Hu, Q.; Hao, W.; Ma, C.; Li, Y.; Yang, B. Products distribution and kinetic analysis on gaseous products during fast pyrolysis of two kinds of biomass pellet. *Fuel* **2019**, *249*, 8–14. [CrossRef]
45. Uddin, M.N.; Daud, W.M.A.W.; Abbas, H.F. Effects of pyrolysis parameters on hydrogen formations from biomass: A review. *RSC Adv.* **2014**, *4*, 10467–10490. [CrossRef]
46. Dhanavath, K.N.; Bankupalli, S.; Sugali, C.S.; Perupogu, V.; V Nandury, S.; Bhargava, S.; Parthasarathy, R. Optimization of process parameters for slow pyrolysis of neem press seed cake for liquid and char production. *J. Environ. Chem. Eng.* **2019**, *7*, 102905. [CrossRef]
47. Pan, R.; Ferreira Martins, M.; Debenest, G. Pyrolysis of waste polyethylene in a semi-batch reactor to produce liquid fuel: Optimization of operating conditions. *Energ. Convers. Manag.* **2021**, *237*, 114114. [CrossRef]
48. Pütün, E. Catalytic pyrolysis of biomass: Effects of pyrolysis temperature, sweeping gas flow rate and MgO catalyst. *Energy* **2010**, *35*, 2761–2766. [CrossRef]
49. Wang, C.; Luo, Z.; Li, S.; Zhu, X. Coupling effect of condensing temperature and residence time on bio-oil component enrichment during the condensation of biomass pyrolysis vapors. *Fuel* **2020**, *274*, 117861. [CrossRef]
50. Papari, S.; Hawboldt, K.; Fransham, P. Study of selective condensation for woody biomass pyrolysis oil vapours. *Fuel* **2019**, *245*, 233–239. [CrossRef]
51. Li, J.D.; Lv, X.Y.; Wang, Y.; Li, Q.X.; Hu, C.W. Hydrotreatment Upgrading of Bio-oil from Torrefaction of Pubescens in Alcohol over Pd/NbOPO4. *Acs Omega* **2018**, *3*, 4836–4846. [CrossRef]
52. Ayanoglu, A.; Yumrutas, R. Rotary kiln and batch pyrolysis of waste tire to produce gasoline and diesel like fuels. *Energ. Convers. Manag.* **2016**, *111*, 261–270. [CrossRef]
53. Nautiyal, P.; Subramanian, K.A.; Dastidar, M.G. Production and characterization of biodiesel from algae. *Fuel Process Technol.* **2014**, *120*, 79–88. [CrossRef]

54. Alagu, R.M.; Sundaram, E.G. Preparation and characterization of pyrolytic oil through pyrolysis of neem seed and study of performance, combustion and emission characteristics in CI engine. *J. Energy Inst.* **2018**, *91*, 100–109. [CrossRef]
55. Knothe, G.; Razon, L.F. Biodiesel fuels. *Prog. Energ. Combust.* **2017**, *58*, 36–59. [CrossRef]
56. Lievens, C.; Mourant, D.; He, M.; Gunawan, R.; Li, X.; Li, C.Z. An FT-IR spectroscopic study of carbonyl functionalities in bio-oils. *Fuel* **2011**, *90*, 3417–3423. [CrossRef]
57. Lozano, D.C.P.; Ramirez, C.X.; Chaparro, J.A.S.; Thomas, M.J.; Gavard, R.; Jones, H.E.; Hernandez, R.C.; Mejia-Ospino, E.; Barrow, M.P. Characterization of bio-crude components derived from pyrolysis of soft wood and its esterified product by ultrahigh resolution mass spectrometry and spectroscopic techniques. *Fuel* **2020**, *259*, 116085. [CrossRef]
58. Uzun, B.B.; Apaydin-Varol, E.; Ates, F.; Ozbay, N.; Putun, A.E. Synthetic fuel production from tea waste: Characterisation of bio-oil and bio-char. *Fuel* **2010**, *89*, 176–184. [CrossRef]
59. Zhou, L.Y.; Yang, H.M.; Wu, H.; Wang, M.; Cheng, D.Q. Catalytic pyrolysis of rice husk by mixing with zinc oxide: Characterization of bio-oil and its rheological behavior. *Fuel Process Technol.* **2013**, *106*, 385–391. [CrossRef]
60. Sakthivel, R.; Ramesh, K.; Shameer, P.M.; Purnachandran, R. Experimental investigation on improvement of storage stability of bio-oil derived from intermediate pyrolysis of Calophyllum inophyllum seed cake. *J. Energy Inst.* **2019**, *92*, 768–782. [CrossRef]
61. Zhang, H.; Liu, X.D.; Li, J.M.; Jiang, Z.C.; Hu, C.W. Performances of Several Solvents on the Cleavage of Inter- and Intramolecular Linkages of Lignin in Corncob Residue. *ChemSusChem* **2018**, *11*, 1494–1504. [CrossRef]
62. David, E.; Kopac, J. Pyrolysis of rapeseed oil cake in a fixed bed reactor to produce bio-oil. *J. Anal. Appl. Pyrolysis* **2018**, *134*, 495–502. [CrossRef]
63. Zhang, R.; Li, L.; Tong, D.; Hu, C. Microwave-enhanced pyrolysis of natural algae from water blooms. *Bioresour. Technol.* **2016**, *212*, 311–317. [CrossRef]
64. Du, X.Z.; Lei, X.M.; Zhou, L.Y.; Peng, Y.; Zeng, Y.; Yang, H.R.; Li, D.; Hu, C.W.; Garcia, H. Bimetallic Ni and Mo Nitride as an Efficient Catalyst for Hydrodeoxygenation of Palmitic Acid. *ACS Catal.* **2022**, *12*, 4333–4343. [CrossRef]
65. Xin, H.; Guo, K.; Li, D.; Yang, H.Q.; Hu, C.W. Production of high-grade diesel from palmitic acid over activated carbon-supported nickel phosphide catalysts. *Appl. Catal. B-Environ.* **2016**, *187*, 375–385. [CrossRef]
66. Noor, C.W.M.; Noor, M.M.; Mamat, R. Biodiesel as alternative fuel for marine diesel engine applications: A review. *Renew. Sust. Energ. Rev.* **2018**, *94*, 127–142. [CrossRef]
67. Huijbers, M.M.E.; Zhang, W.Y.; Tonin, F.; Hollmann, F. Light-Driven Enzymatic Decarboxylation of Fatty Acids. *Angew. Chem. Int. Ed.* **2018**, *57*, 13648–13651. [CrossRef]
68. Duong, H.T.; Wu, Y.Q.; Sutor, A.; Burek, B.O.; Hollmann, F.; Bloh, J.Z. Intensification of Photobiocatalytic Decarboxylation of Fatty Acids for the Production of Biodiesel. *ChemSusChem* **2021**, *14*, 1053–1056. [CrossRef]
69. Wei, G.T.; Liu, Z.H.; Zhang, L.Y.; Li, Z.M. Catalytic upgrading of Jatropha oil biodiesel by partial hydrogenation using Raney-Ni as catalyst under microwave heating. *Energ. Convers. Manag.* **2018**, *163*, 208–218. [CrossRef]
70. Chen, B.S.; Zeng, Y.Y.; Liu, L.; Chen, L.; Duan, P.G.; Luque, R.; Ge, R.; Zhang, W.Y. Advances in catalytic decarboxylation of bioderived fatty acids to diesel-range alkanes. *Renew. Sust. Energ. Rev.* **2022**, *158*, 112178. [CrossRef]
71. Chen, W.; Fang, Y.; Li, K.X.; Chen, Z.Q.; Xia, M.W.; Gong, M.; Chen, Y.Q.; Yang, H.P.; Tu, X.; Chen, H.P. Bamboo wastes catalytic pyrolysis with N-doped biochar catalyst for phenols products. *Appl. Energ.* **2020**, *260*, 114242. [CrossRef]
72. Murray, I. *Methods in Agricultural Chemical Analysis, A Practical Handbook, by N. T. FAITHFULL. xxii+266 pp. Wallingford: CABI Publishing. £60.00 (hardback). ISBN 0 85199 608 6*; Cambridge University Press: Cambridge, UK, 2003; Volume 140, p. 249.
73. Qi, W.Y.; Hu, C.W.; Li, G.Y.; Guo, L.H.; Yang, Y.; Luo, J.; Miao, X.; Du, Y. Catalytic pyrolysis of several kinds of bamboos over zeolite NaY. *Green Chem.* **2006**, *8*, 183–190. [CrossRef]
74. Friedl, A.; Padouvas, E.; Rotter, H.; Varmuza, K. Prediction of heating values of biomass fuel from elemental composition. *Anal. Chim. Acta* **2005**, *544*, 191–198. [CrossRef]